Computational Materials Science 111 (2016) 116–124

Contents lists available at ScienceDirect

Computational Materials Science

journal homepage: www.elsevier.com/locate/commatsci

Multi-cycle and multi-scale cellular automata for hydration simulation (of Portland-cement)

H.J.H. Brouwers, A.C.J. de Korte *

Department of the Built Environment, Eindhoven University of Technology, P.O. Box 513, 5600 MB Eindhoven, The Netherlands

ARTICLE INFO

Article history:
Received 10 June 2015
Received in revised form 24 August 2015
Accepted 26 August 2015
Available online 24 September 2015

Keywords:
Hydration
Kinetics
Portland cement
Modelling
CEMHYD3D
System resolution

ABSTRACT

CEMHYD3D is a cellular automata (or agent) based computer model for the hydration of cementitious materials, which is able to predict the microstructure and physical properties of such hydrating systems. In this paper, CEMHYD3D is successfully extended for multi-cycle and multi-scale modelling. Multi-cycle means the possibility to zoom in and out on the hydration process with respect to time. Multi-cycle modelling enables the user to study the hydration in more detail in both the early phase (minutes) and on the long term (years). This modelling is needed, for instance to be able to model the hydration of reactants with different reaction rates (e.g. Portland cement and calcium sulphates). The multi-scale modifications enable the use of smaller particles than the standard minimum size of 1 μm, which permits the incorporation of submicron particles in the model. These particles are present in most cementitious binders, and their inclusion will improve the predictions of properties during simulation.

Based on statistical considerations, the dissolution and nucleation probabilities and the number of diffusion steps from the original model have been modified in order to enable multi-scale and multi-cycle modelling. For the multi-scale, two variants to obtain the microstructure at higher resolution have been applied, voxel splitting and rescaling, which differ in the way they deal with the particle shape.

All modifications have been tested for the modifications separately as well as both combined, for a system consisting of an OPC cement, using CEMHYD3D. All simulations showed good agreements between the results at different resolutions (for both scaling methods) and applying different time-steps, confirming the validity of the generally applicable equations presented here.

1. Introduction

Hydration models are used to reduce the number of the real tests needed to optimize a mix design. Examples of these hydration models are CEMHYD3D [1], HYMOSTRUC [2], the Navi and Pignat model [3], μic [4] and HydratiCA [5,6]. These models are able to represent the physical properties and present reaction mechanism during hydration. As pointed out by Chen and Brouwers [7], the physical properties of a hydrating microstructure are limited by the smallest element-size available in the system, the so-called system resolution. Besides the representation of the properties, the system resolution also influences the needed computation power and time needed to run a simulation. In this paper it is shown that resolutions of 0.2 μm nowadays are possible due to increased computations power, while in the original version of CEMHYD3D the used resolution is 1 μm. The use of lower resolutions leads to problem that the amount of hydrated cement per cycle decreases when the system resolution increases [8] and therefore the predictions of the models significantly depend on the system resolution. Garboczi and Bentz [8] discuss the required resolution needed and concluded that 0.2 μm is sufficient. Chen and Brouwers [7] have incorporated the diffusion layer system of Van Breugel [2] into the CEMHYD3D-model.

This paper intends to improve the predictions of the CEMHYD3D model for different system resolution (different scales) by further modification of the dissolution and nucleation probability and the number of diffusion steps within the model. The CEMHYD3D is chosen because of it is believed to be one of the most advanced, well-known and most widely-used computer hydration models [2,4].

Besides the multi-scale modelling, this paper also pays attention to multi-cycle modelling. Multi-cycle modelling enables to zoom in and out into hydration process with regard to time. This is needed for instance when one wishes to study the hydration of calcium sulphate hemihydrates, which have a extreme short hydration time compared to cements, or when one wishes to study

* Corresponding author. Tel.: +31 40 247 3350; fax +31 40 243 8595.
E-mail address: a.c.j.dekorte@gmail.com (A.C.J. de Korte).

http://dx.doi.org/10.1016/j.commatsci.2015.08.049
0927-0256/

the long-term reaction behaviour of cementitious materials, when the reaction rate becomes extremely slow.

Both modifications will lead to modifications in the modelling of the hydration process, which consists of dissolution, diffusion and nucleation stage of the process.

2. CEMHYD3D: a 3-D computer-based hydration model

The computer model CEMHYD3D was originally developed by Bentz and Garboczi [9] to represent the hydration process of Portland cement in two-dimensions. Later on, the model was later extended to a 3D-computermodel and other cementitious materials, like fly-ash and silica fume, as reactants were included [10]. Van Eijk [11] has calibrated the model with two Dutch cements CEM I 32.5R and 52.5R, and introduced pore water chemistry. Chen [12] and Chen et al. [13] have introduced slag blended cement into the hydration model including the new phases and their reactions as well as the difference in reactivity between cement and slag material. Furthermore further improvements were done in order to overcome some side effects of changing system resolution. At last mineral shrinkage compensating mixtures were designed by Chen and Brouwers [7] and Chen [12] based on simulations and real tests. Bentz [14] compared CEMHYD3D and real 3-D X-ray microtomography cement paste microstructures using correlation functions. Igarashi et al. [15] compared the simulated microstructures of CEMHYD3D with SEM-BSE image analysis of cement pastes microstructures. Smilauer [16] studied the elastic properties of hydrating cement paste by applying elastic homogenization methods on the microstructures provided by CEMHYD3D. Koster [17] uses CEMHYD3D for the simulation of 3-dimensional moisture transport through and moisture absorption by capillary-porous building materials. Feng et al. [18] uses the initial microstructure provided by CEMHYD3D to simulate the influence of leaching on hydrated cement pastes. Robeyst et al. [19] related the fundamental changes in the microstructure, noticed using ultrasonic measurement during the setting of concrete, with the microstructure development simulated by CEMHYD3D. Newest developments introduced by NIST can be found in the work of Bentz [14,20–22].

The CEMHYD3D-model usually represent the microstructure of hydrating cement by using a $100 \cdot 100 \cdot 100$ box with 10^6 voxels of size $1 \cdot 1 \cdot 1$. Other resolutions are possible to use, although larger system sizes and smaller voxel sizes represent the microstructure more accurately, the computing time needed for these system and voxel sizes is remarkably higher. According to Smilauer and Bittnar [23], the reasonable microstructure size lies in the range of 20–50 μm and a microstructure edge size above 100 μm has been found to bring no significant accuracy in the hydration model predictions. Garboczi and Bentz [8] point out that 0.2 μm resolution is accurate enough for simulation of cement hydration. Therefore in this paper a microstructure of $100 \cdot 100 \cdot 100$ μm^3 is used while a system resolution up to 0.2 μm is tested.

The particles within the initial microstructure are created by placing voxels in an approximately spherical shape called "digitized particle" within the box. A 1-μm particle in CEMHYD3D is represented by 1 voxel at a system resolution of 1 μm, while at a system resolution of 0.33 μm it is represented by 19 voxels with size of 0.33 μm. An example for the digitized particle of size 1, 3, 5, 7, 11 and 21 voxels is shown in Fig. 1, which contain 1, 19, 81, 179, 739 and 4945 voxels, respectively.

In the original version of CEMHYD3D only phase-boundary-reaction (chemical reaction controlled) was considered. According to Chen [12], the diffusion layer is needed in order to correct for the effect of the system resolution. He incorporated the diffusion layer into the CEMHYD3D-model, based on the work done by Van Breugel [24]. Van Breugel [24] showed that the reaction rate is constant for phase-boundary reaction and decreasing for diffusion controlled circumstances. The transition point between both mechanism is defined by layer thickness δ_{tr}. This is shown in Fig. 3. Both mechanism and the transition layer have been incorporated by Chen [12] and Chen and Brouwers [7]. The dissolution probability is an complicated function depending on temperature, reaction degree, sulphate concentration and other parameters. For readability here for the description of dissolution probability function, $P_{D,1}$ is used. $P_{D,1}$ includes the earlier mentioned parameters. The dissolution probability for the phase-boundary reaction reads;

$$P_{D,1} = P_{D,0} \quad \text{for } \delta \leqslant \delta_{tr} \tag{1}$$

and the dissolution probability for the diffusion controlled part, based on Chen [12] and Chen and Brouwers [7], reads;

$$P_{D,1} = P_{D,0} \cdot \frac{\delta_{tr}}{\delta} \quad \text{for } \delta > \delta_{tr} \tag{2}$$

with $P_{D,0}$ the basic dissolution probability function (here presented as an constant value, but in fact an complicated function), δ the layer thickness and δ_{tr} the theoretical transition layer thickness. According to van Breugel [24], the transition layer thickness for low heat cement equals 2–4 μm and for fast hydrating cements 3–6 μm. In CEMHYD3D a δ_{tr} of 2 μm is chosen [7,13]. A full description of CEMHYD3D can be found in [7,10,25].

3. Multi-cycle modelling

In this section, the option of multi-cycle modelling is introduced. The idea behind multi-cycle is the variation of the length of the time steps in the model. Fig. 2 shows the principle of multi-cycle modelling. In this section the term reference cycle will be used to describe a cycle within the original model. In order to describe this variation, the multi-cycle factor k is introduced. A higher multi-cycle factor results in k smaller time steps during hydration and therefore resulting in k time more cycles to achieve a same degree of hydration. Hence, for a reference cycle holds that $k = 1$.

This is necessary, because the hydration of some reactants, e.g. hemihydrate, may be much faster compared with the hydration of the cement clinkers. The complete hydration of hemihydrate takes place within half an hour, while cement takes a few days. Multi-cycle modelling introduces two major adaptations to the model: the modification of the reaction kinetics and a correction of the calculation of the reaction time.

Within CEMHYD3D the kinetics are mainly regulated by the dissolution and nucleation probabilities and the number of diffusion steps. Due to smaller time step at a larger k-factor, the number of particles that dissolve, diffuse and nucleate is smaller. Therefore these probabilities need to be smaller. In this section, the modification of the reaction kinetics is described. In this paper the reference system refers to the system with system resolution of 1 μm and without any multi-scale (nor multi-cycle) modifications.

3.1. Dissolution

The expectation of a voxel-face to dissolve in the reference system during a cycle equals the dissolution probability ($P_{D,1}$). In general, for k cycles the expectation reads

$$\sum_{i=0}^{k} i \left[\binom{k}{i} P_{D,k}^{k-i} (1 - P_{D,k})^k \right] = k P_{D,k} \tag{3}$$

With $P_{D,k}$ is the dissolution probability when a cycle is divided into k new cycles. This probability is equal to the expectation of dissolution in the reference system, $P_{D,1}$, when

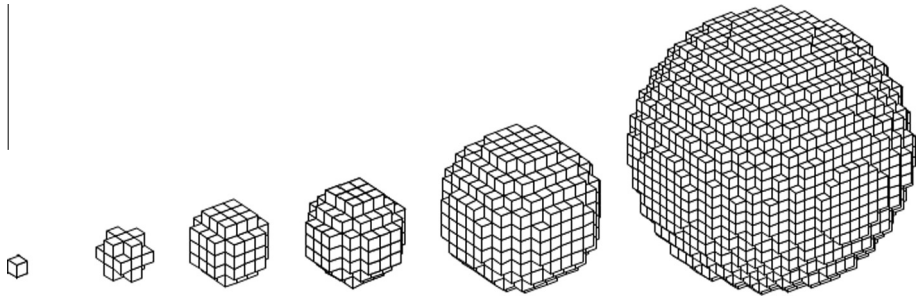

Fig. 1. Digitized particle with sizes of 1, 3, 5, 7, 11 and 21 voxels.

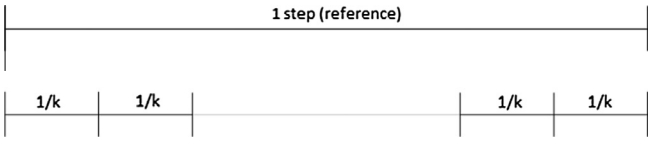

Fig. 2. Schematic representation of the reference cycle and the multi-cycle cycle ($k > 1$).

$$P_{D,k} = \frac{1}{k} P_{D,1} \tag{4}$$

with k is the multi-cycle factor.

3.2. Diffusion

As described earlier, in Section 2, diffusion is modelled as a series of random walks. In the present model 500 random diffusion steps (D_1) are undertaken. After every diffusion step, there is a possibility for nucleation. The average distance according to literature [26–28] reads;

$$\langle d \rangle = l_0 \cdot \sqrt{D_1} \tag{5}$$

With ⟨d⟩ the average distance, l_0 the average step size and D_1 the number of steps. When it is assumed that a voxel can walk in 1 cycle over a distance $\langle d \rangle$, and multi-cycle modelling will not change the speed and step size (l_0) of a voxel, then in multi-cycle situation after k cycles the same distance $\langle d \rangle$ should be travelled. Therefore the number of diffusion steps (D_k) during one new cycle reads;

$$D_k = \frac{1}{k} \cdot D_1 \tag{6}$$

3.3. Nucleation

Nucleation is the third reaction mechanism. If $P_{N,1}$ is the nucleation probability for $k = 1$ and $P_{N,k}$ is the nucleation probability for 1 cycle in the situation of k cycles. Similar to the dissolution probability, the nucleation probability reads;

$$P_{N,k} = \frac{1}{k} P_{N,1} \tag{7}$$

3.4. Cycles correction

The multi-cycle modification influences both the number of cycles and the reaction rate. Since the reaction rate depends on the temperature and the reactions (dissolution and nucleation) in the model directly influence the temperature, no modification is needed here. On the other hand, the number of cycles needs to be modified. The number of cycles in the reference system can calculated from the number of cycles in the multi-cycle systems. The correction consists of two parts. The first part is the correction for the step size. Instead of 1 cycle in the reference situation, k cycles are carried out in the multi-cycle situation. The second correction is a correction for the starting point. Instead of starting with cycle 0, the new situation starts with cycle $2–2/k$. So the calculation of cycles in according to the following equation;

$$C_1 = C_k \cdot \frac{1}{k} + \left(2 - \frac{2}{k}\right) \tag{8}$$

With C_k the number of cycles in the multi-cycle situation and C_1 the cycles in the original system. The time can be calculated based on the C_1 using the standard relation between time and cycles for CEMHYD3D. The time conversion factor does not have to be changed for multi-cycle modification, since this is accounted for by Eq. (8).

4. Multi-scale modelling

Chen [12] and Chen and Brouwers [7] pointed out that the smallest size handled in CEMHYD3D, called the 'system resolution', is an important feature of a digitized model. Particles smaller than the 1 μm voxel size cannot be represented since the model is based on the movement and phase change of each discrete voxel. Furthermore, the system resolution determines the amount of computing time needed for a specific task, a higher system resolution will lead to a longer computational time. Due to better computation possibilities, the use of higher resolutions is possible nowadays. Chen [12] already presented the simulations with resolutions from 0.5 to 2 μm. In this research the model has been further modified to cope with several different resolutions from 0.2 to 2 μm (or 500^3 to 50^3 voxels in the system).

Chen [12] and Chen and Brouwers [7] indicate that the absence of diffusion controlled reaction mechanism in the original version of CEMHYD3D leads to undesired effects of system resolution on the model predictions. Changing the system resolutions will change the model outcome significantly [8], which will not be the case in a robust system. Therefore Chen [12] included diffusion controlled reaction mechanism in the CEMHYD3D-model. The next section will describe the necessary modification needed for the multi-scale modification.

4.1. Modification of the hydration system

The initial microstructure at a resolution of 1 μm is created with the Makecem-module of CEMHYD3D, while the microstructure at other (lower) resolutions is created by splitting the voxels in the microstructure into more elements or by rescaling the particles. Fig. 3a shows a voxel at resolution of 1 μm, while Fig. 3d shows the same voxel at resolution of 0.33 μm by voxel splitting. The simplest case of 1 voxel particle that is split in a particle containing 8 voxels of size 0.5 is treated as example here (Fig. 3b).

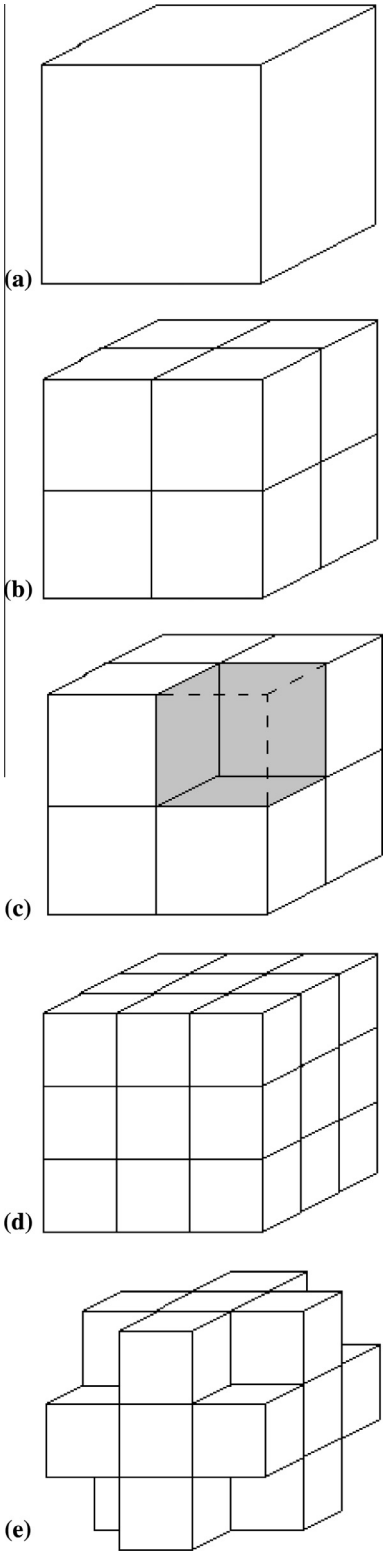

Fig. 3. Schematic representation of the principles of voxel splitting (b–d) and rescaling (e) for multi-scale modelling using a 1 voxel size particle (a). In (c) the blocked faces in case of dissolution in version A of CEMHYD3D are shown in grey.

The probability that particle consisting of one voxel does not dissolve in one cycle reads

$$1 - P_{D,p1} = (1 - P_{D,0})^6 \tag{9}$$

with $P_{D,0}$ as the dissolution probability of one particle (voxel) face in the reference system, and $P_{D,p1}$ is the dissolution probability of the entire particle, which has 6 faces (Fig. 5a). When the particle consists of 8 voxels of size 0.5, each voxel has 3 external faces (Fig. 5b). Hence, the probability one individual voxel will not dissolve follows as

$$1 - P_{D,v2} = (1 - P_{D,2})^3 \tag{10}$$

with $P_{D,2}$ as the dissolution probability of each 0.5 voxel face in the system with double resolution, and $P_{D,v2}$ is the dissolution probability of each voxel.

The probability that none of the 8 voxels dissolves is $(1 - P_{D,v2})^8$ and that all 8 voxels (i.e. the entire particle) dissolve is $(P_{D,v2})^8$. In general, the probability that i voxels dissolve is $\binom{8}{i} D_{D,v2}^{8-i}$ $(1 - D_{D,v2})^i$. The overall probability for the dissolution of the 8 voxel particle reads:

$$P_{D,p2} = \sum_{i=0}^{8} \left[\binom{8}{i} P_{D,v2}^{8-i} (1 - P_{D,v2})^i \left(\frac{i}{8} \right) \right] = P_{D,v2} \tag{11}$$

The 1 voxel and 0.5 voxel systems are congruent when $P_{D,p2} = P_{D,v2}$ equals $P_{D,p1}$, hence yielding as expression

$$P_{D,s} = 1 - (1 - P_{D,0})^s \tag{12}$$

with $s = 2$, i.e. as the number that governs the split of each voxel. Without further proof it is assumed that the derivation for $s = 2$, presented in the foregoing, also holds for other resolution increases, so $s = 3$, 4, etc.

4.2. Diffusion layer

In the previous subsection, the multi-scale modification for the surface controlled reactions are described. This subsection will extend this modification to diffusion controlled system. Eq. (2) described the reaction probability for diffusion controlled part in the reference system. When assuming that the probability changes in the same manner as for the surface-based dissolution (Section 4.1, Eq. (12)), the modified equation for the diffusion controlled part becomes;

$$P_{D,s} = \left(1 - (1 - P_{D,0})^s\right) \frac{\delta_{tr}}{\delta} \tag{13}$$

with δ the diffusion layer thickness, δ_{tr} the transition layer thickness, s the multi-scale factor. To obtain the same (transition) layer thickness and layer thickness at different resolutions, the number of voxels differ. Fig. 4 shows a graphical representation of the diffusion layer thickness (δ) at different resolutions. Fig. 4a shows diffu-

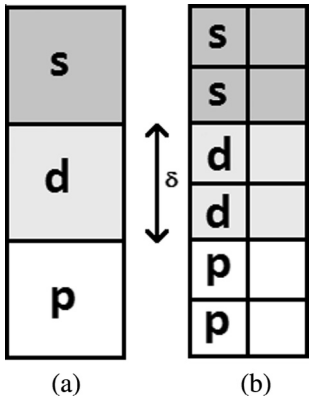

Fig. 4. A graphical representation of the diffusion layer thickness at different resolutions with S the source (cement) voxel, d the diffusion layer voxel and p the void fraction voxel. In the example, (a) the reference system with a diffusion layer of 1 voxel and (b) a $s = 2$ system, in which the diffusion layer consists of two voxels.

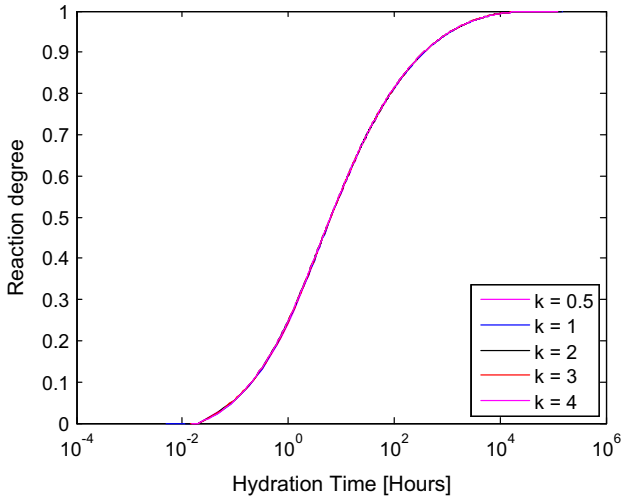

Fig. 5. Multi-cycle simulation of the CCRL-116 (Table 2) with PSD (Table 1) and a water–binder ratio of 1.2.

Table 1
The used particle size distribution for simulations.

Particle size (μm)	Volume fraction (% V/V)
1	0.0
3	0.0
5	10.8
7	20.8
9	14.4
11	10.8
13	8.5
15	6.5
17	5.2
19	4.1
21	3.2
23	2.6
25	2.5
27	2.3
29	2.2
31	2.1
33	1.1
35	1.0
37	1.0
39	0.9

Table 2
Chemical composition of the 'used' CCRL-116 cement [31].

Cement clinker	Mass fraction (% m/m)
C_3S	67.08
C_2S	22.17
C_3A	7.11
C_4AF	3.64

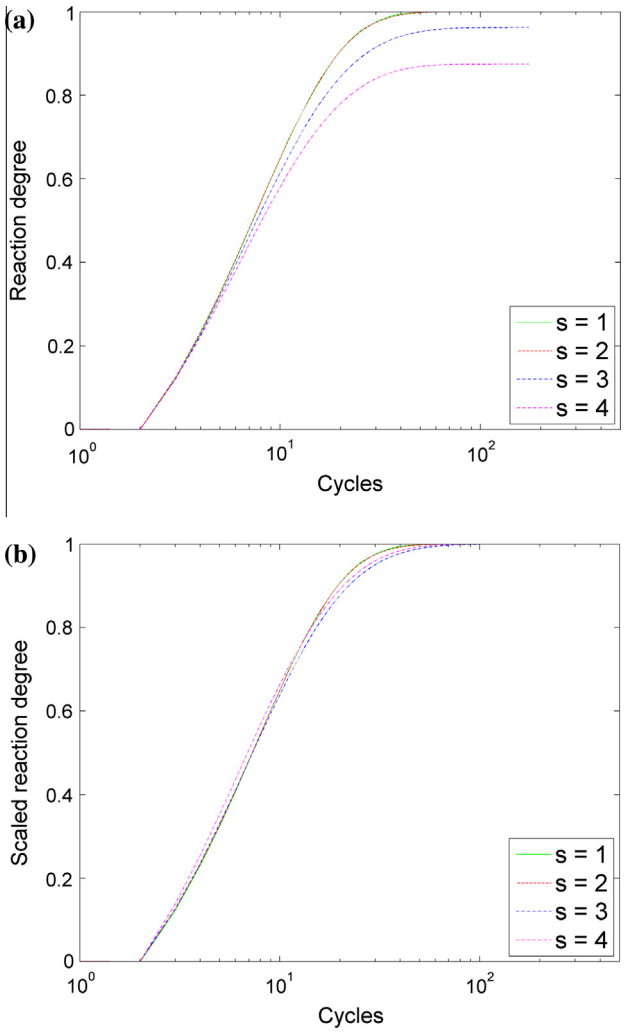

Fig. 6. Hydration curves showing the results of applying/validating the derivation of Eq. (12) using as dilute system (wbr = 12.64) with 1 μm particles (without deposition of reaction products).

sion layer at the reference system ($s = 1$) and Fig. 4b shows the layer at $s = 2$. Whereas on the left side the diffusion layer is formed by one voxel, on the right side two voxels are needed. So the number of voxels to reach a diffusion layer thickness δ is proportional to s and reciprocal to the resolution.

Besides the dissolution probability also the number of diffusion steps and nucleation chance need to be adapted. The average distance that a voxel moves during a random walk needs to be the same at different resolutions. The average distance is given by Eq. (5). Assuming that distances at different resolutions needs to be equal and the average step size is equal to $1/s$, the following relation between number of diffusion steps then reads

$$D_s = s^2 \cdot D_1 \tag{14}$$

With D_1 the original number of steps and s the multi-scale factor. The modified nucleation probability equation reads

$$P_{N,1} = P_{N,0} \cdot \left(1 - e^{-\frac{i_1}{i_{\max,0} \cdot s^3}}\right) \tag{15}$$

with i_1 is the number of diffusing voxels, $P_{N,0}$ the nucleation chance without multi-scale and multi-cycle, $i_{\max,0}$ the scale factor for nucleation for the 1 μm reference system, and s the multi-scale factor. The factor s^3 in Eq. (15) can be explained by the fact the total number of voxels in the system increases by this factor compared to the reference system.

4.3. Combined multi-scale and multi-cycle modelling

The previous sections describe the modifications for multi-cycle and multi-scale modelling separately. This section addresses the combination of both modifications. In case of surface-controlled

Table 3
Properties of phases used in CEMHYD3D [11,12].

Name	Density ρ (g/cm^3)	Molar volume ω (cm^3/mol)	Molar mass M (g/mol)	Heat of formation (kJ/mol)	Dissolution probability $P_{D,0}$ (–)	Nucleation probability $P_{N,0}$ (–)	Nucleation scale factor $i_{max,1}$ (–)
C_3S	3.21	71	228	−2928	0.027		
C_2S	3.28	52	171	−2312	0.005		
C_3A	3.03	89.1	270	−3588	0.027		
C_4AF	3.73	128	477	5090	0.003		
$C\bar{S}H_2$	2.32	74.2	172	−2023	0.0017	0.01	90,000
$C\bar{S}H_{0.5}$	2.73	53.2	145	−1575	0.005		
$C\bar{S}$	2.61	52.2	136	−1425	0.001		
$C_{1.7}SH_{4.0}$	2.12	108	229	−3283		0.01	100,000
$C_{1.1}SH_{3.9}$	1.69	101.8	172	−2299		0.01	100,000
CH	2.24	33.1	74	−986		0.01	20,000
$C_6A\bar{S}_3H_{32}$	1.7	735	1250	−17,539			
$C_4A\bar{S}H_{12}$	1.99	313	623	−8778			
C_3AH_6	2.52	150	378	−5548			
C_4AH_{13}	2.04	273	560	−8318	0.0167	0.002	10,000
FH_3	3.69	8	209	−824		0.2	2500
MH	2.39	24	58	−924		0.6	2500
S	2.2	27	59	−908			
H	1	18	18	−286			

Table 4
Used versions of the model.

Purpose	Version A validation derivation	Version B full model
Diffusion layer	Impermeable	Yes
Surface precipitation	No	Yes
Spontaneously nucleation	No	Yes
Cement composition	C_3S	OPC
Particle size distribution	Mono-sized (1 μm)	Polydisperse
Water/binder ratio	Dilute (12.65)	Normal

reaction (so no diffusion layer) the equation for the dissolution probability, assuming both modification are not correlated, reads;

$$P_{D,k,s} = 1 - \left(1 - \frac{1}{k} P_{D,0}\right)^s \quad \text{for } \delta \leqslant \delta_{tr} \tag{16}$$

While the equation for diffusion controlled part reads;

$$P_{D,k,s} = \left(1 - \left(1 - \frac{1}{k} P_{D,0}\right)^s\right) \cdot \frac{\delta_{tr}}{\delta} \quad \text{for } \delta > \delta_{tr} \tag{17}$$

In both cases the number of diffusion steps is equal to

$$D_{k,s} = \frac{1}{k} \cdot s^2 \cdot D_1 \tag{18}$$

5. Simulation results

5.1. Multi-cycle simulations

In Section 3, the modifications of CEMHYD3D in case of multi-cycle simulations were described. These modifications included the modification of all three main hydration process steps, namely dissolution, diffusion and nucleation. This involved the modification of the dissolution and nucleation probability, the number of random walk diffusion steps as well the correction of the number of cellular automata cycles. In this subsection, all modifications are validated.

For the validation of the multi-cycle modifications, a mixture of Portland cement and water with a water–binder ratio of 1.2 was used. The applied Portland cement was CCRL cement 116 [29–31]. Table 1 shows the particle size distribution used for the multi-cycle simulations. The clicker composition of the used CCRL-116 cement can be found in Table 2. The cellular automata parameters, such as specific density, dissolution and nucleation probabilities of the different cement phases, used for the simulations are presented in Table 3.

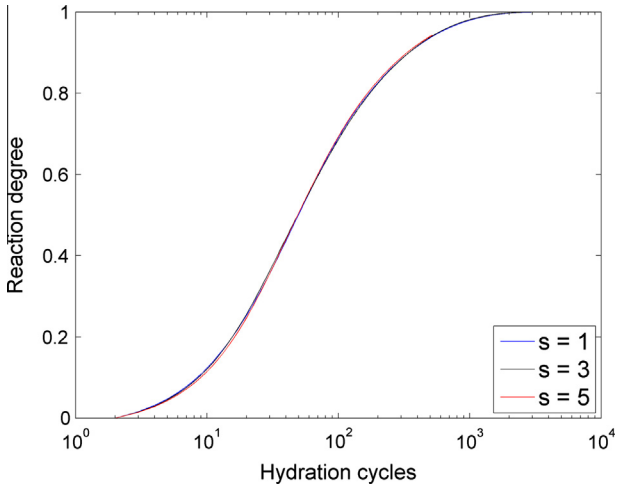

Fig. 7. The results of multi-scale simulation of the CCRL-116-cement (Table 2) with full particle size distribution (Table 1) and a water–binder ratio of 1.37 using the voxel splitting method.

Fig. 5 shows the hydration curve for a OPC with diffusion layer for several multi-cycle factors k for system. The difference between the dissolution lines is very small, confirming the validity of the newly derived equations for dissolution probability, the number of diffusion steps and nucleation probability, Eqs (4), (6) and (7), respectively. The figure also shows that the correction of the cycles using Eq. (8) is valid.

Furthermore it can be concluded from Fig. 5, that the multi-cycle modification can be applied both for zooming in and out with regard to cycles/time. This features enables the possibility to study very fast hydrations, like calcium sulphates as well as the study of the long term hydration behaviour of cementitious materials.

5.2. Multi-scale by voxel splitting

In order to verify the multi-scale model, Eq. (12) is tested within version A of CEMHYD3D (see Table 4). This version of the system consists of a dilute system with dispersed 1 μm voxels (2.47% V/

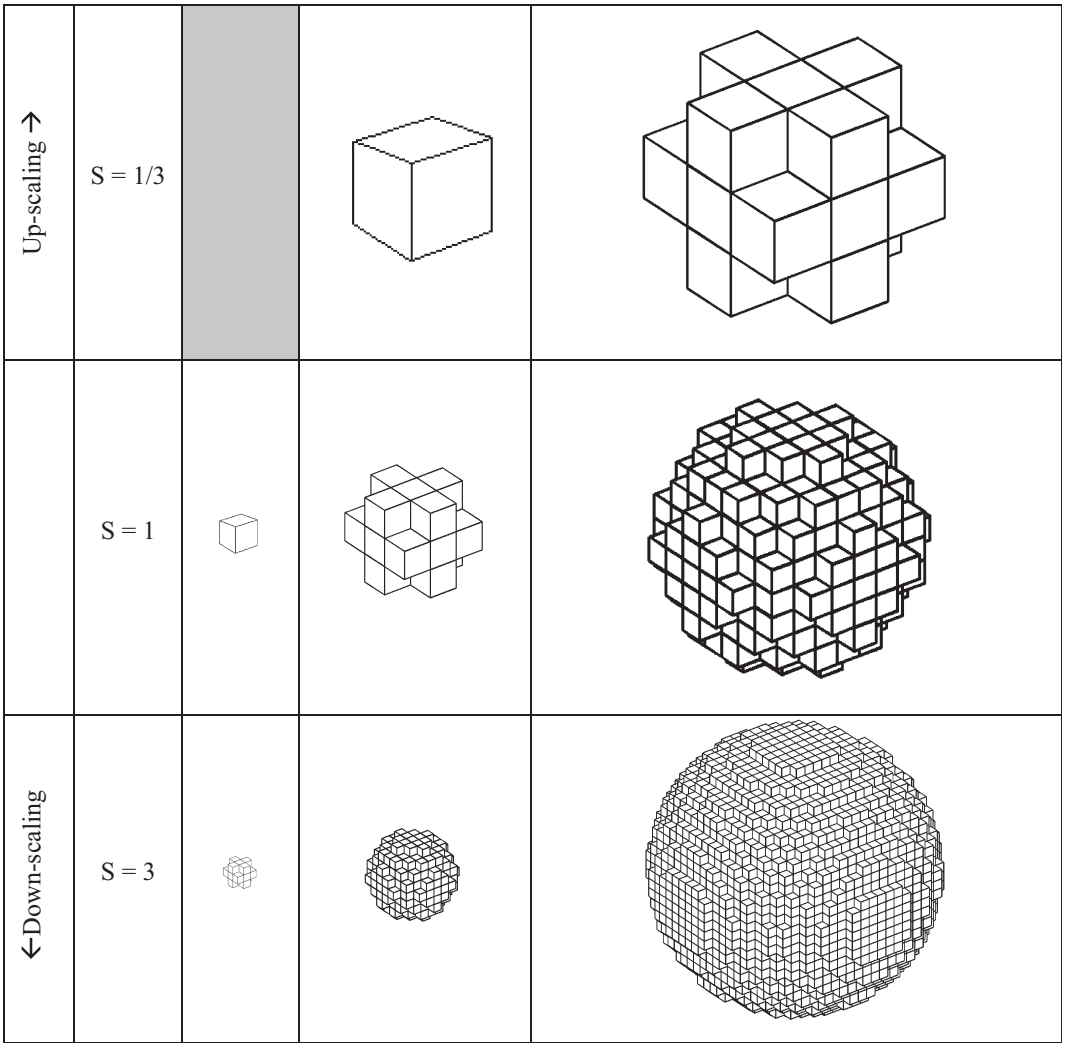

Fig. 8. Schematic representation of the principle of up- and downscaling of 1, 3 and 9 particle (at $s = 1$, reference system) with $s < 1$ for downscaling and $s > 1$ for upscaling.

V) with a minimum distance of 2 μm, so no diffusion layers nor precipitation of hydration products are considered and each voxel which dissolves creates an impermeable voxel keeping shared sites of other voxels insoluble. In Fig. 3c, the shared insoluble voxel faces are shown in grey in case the top right voxel is dissolved.

Fig. 6a shows the simulation results for this test case. As can be noticed from the figure, the hydration lines for $s = 1$ and $s = 2$ are almost identical. Therefore this case is confirming the derivation presented in Section 4.1. The hydration curves for $s = 3$ and $s = 4$ reach a lower final hydration degree, which can be explained by the fact that voxels in the middle of particles are blocked for dissolution by the surrounding particles. The theoretical maximum hydration degree due to blocking of these internal voxels is 26/27 (~ 0.963) and 56/64 ($= 0.875$) for $s = 3$ and $s = 4$, respectively. When one takes into account the theoretical maximum hydration degree, the hydration curves for $s = 3$ and $s = 4$ behave as expected, although some effects of the fact that the outer layer consists of voxels with 1, 2 and 3 surfaces exposed to the pore solution, are visible (Fig. 6b).

Eq. (12) has been validated using version A of CEMHYD3D (Table 4) for several resolutions. In reality this simplified system does not exist, since dissolution creates additional reaction surfaces and leads to the formation of hydration products through which the cement can diffuse. Here this simplified system (version A) will be extended with the creation of additional reaction surface by not blocking the shared sides of voxels and allowing for the creation of hydration products which can precipitate on the particle and spontaneously nucleate in the pore solution. The extended cement hydration model (version B) including Eq. (13) is used in this section. The new (dissolution) routine, which was introduced

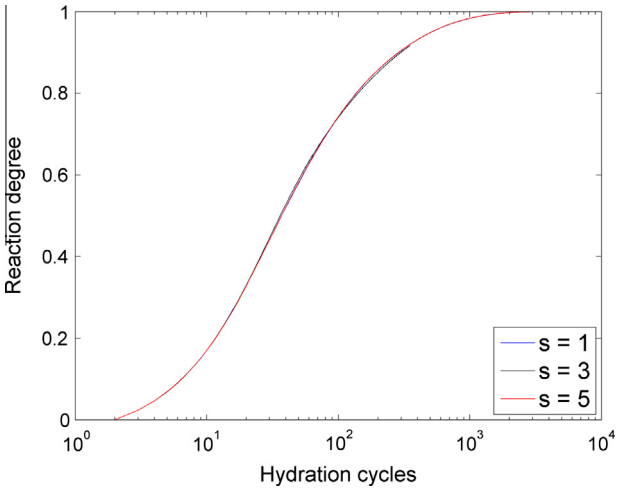

Fig. 9. The results of multi-scale simulations of the CCRL-116-cement (Table 2) with a particle size distribution (Table 1) and a water–binder ratio of 0.6 using the rescaling method.

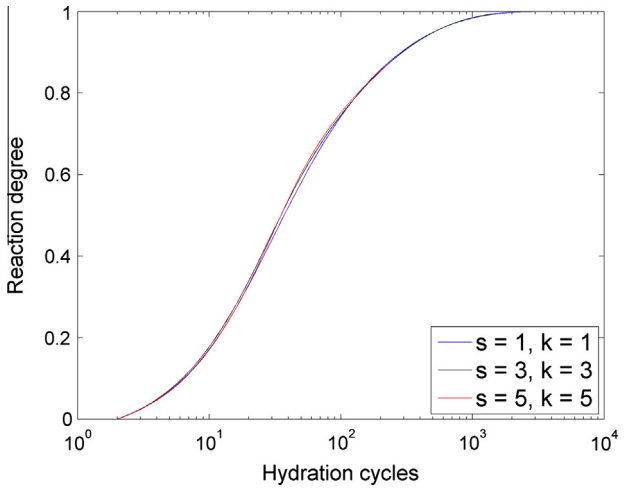

Fig. 10. The results of a combined multi-scale and multi-cycle simulation of CCRL-116-cement (Table 2) with a particle size distribution (Table 1) and a water–binder ratio of 0.6 using the rescaling method.

in De Korte and Brouwers [25,32], has been incorporated in this (extended) version B of CEMHYD3D. The main difference between the original and the new (dissolution) routine is that the new routine tries to maintain the spherical shape of the particles and therefore its dissolution behaviour is closer to the shrinking core theory, since the creation of additional reactive surface, due to the discrete manner of cellular automata, is partially prohibited.

Fig. 7 shows the reaction degree during hydration of CCRL Portland cement 116 with a water–binder ratio of 1.37. The clinker composition of this cement can be found in Table 2 and the used particle size distribution is given in Table 1. One can notice from Fig. 7 that the derived multi-scale modifications (Eqs. (12) and (13)) can be successfully applied using the voxel splitting method (Fig. 3b and d) for the multi-scale simulation of Portland cement.

5.3. Multi-scale by particle rescaling

Another possibility to simulate the hydration at higher resolutions is rescaling instead of voxel splitting. Fig. 8 shows the principle of both the up and down-scaling for a 1, 3 and 9 particle with a factor of three. With downscaling, a 3-particle is used to represent a 1 μm-particle in a $s = 3$ system, a 9-particle is used for 3 μm particle and so on. The difference of downscaling compared to voxel splitting is that particles are becoming more spherically shaped.

During this simulation, the number of particles of the different sizes is kept the same at different resolutions. This ensures that the particle size distribution remains the same, but it has a slight effect on the volume ratio of the binder. Furthermore downscaling would enable the possibility to use a smaller minimum particle size, which is beyond the scope of this paper.

As one can notice from Fig. 8, in case of up-scaling, there is a challenge in order to represent a 1 μm particle, since no digitized particle is available for this size. A solution for this could be a redesign of the particle size distribution.

Fig. 9 shows the results of hydration using downscaling of the CCRL 116 Portland cement with a water/binder-ratio of 0.6. Tables 1 and 2 present the used particle size distribution and the clinker composition of the applied Portland CCRL 116 cement, respectively. Table 3 shows the cellular automata parameters, such as specific density and dissolution probability of the different cement phases, which were used during the simulation. The figure reveals that with the current multi-scale model different system resolutions can be successfully transformed into each other. This provides the opportunity to use a larger size range than was available in the original version of CEMHYD3D. For example for $s = 3$ downscaling, instead of 1 μm particle as minimum particle size now 1/3 μm particle are allowed in the system. This size is actually very close to the smallest particle size found in cements, calcium sulphates, and other cementitious materials [33].

5.4. Combined multi-cycle and multi-scale

In Sections 5.1–5.3, the multi-cycle and multi-scale modifications were tested separately. In this subsection, both modifications are applied simultaneously. This is tested using a mixture containing CCRL-116 Portland cement with a water–binder ratio of 0.60. The particle size distribution and clinker composition listed in Tables 1 and 2, respectively, were used. The used dissolution probabilities and other cellular automata parameters are again taken from Table 3.

Fig. 10 shows the simulation results of the three tested combinations of multi-cycle and multi-scale factors, k and s, respectively. The first combination is the so-called reference case, in which $s = 1$ and $k = 1$ (e.g. no modifications). The second combination is the 300 system (i.e. a system resolution of 0.33 μm) with 1/3 time steps ($s = 3$, $k = 3$) and the third combination is a 500 system (0.2 μm) with 1/5 time steps (so $s = 5$, $k = 5$). As one can notice from the figure, there is only a slight deviation between all combinations, but the difference is minor. In other words, both multi-cycle as multi-scale features presented, can be used to model cellular automata systems. These features extend the CEMHYD3D model with the possibility to zoom in and out in both time/cycles as well as particle size range at the same time.

6. Conclusions

This paper focuses on the modification/extensions of cellular automata (or agent) based models with multi-cycle and multi-scale features, using the CEMHYD3D cement hydration model as example. The main purpose of these extensions is to be able to study the properties of cementitious materials during hydrating with smaller time-steps (multi-cycle) and at higher resolutions (multi-scale). Therefore the dissolution and nucleation probabilities and the number of diffusion steps from the original model have been modified based on statistical considerations. For the multi-scale modifications, two variants to obtain the microstructure at higher resolutions have been applied, namely voxel splitting and rescaling. The main difference between both methods is the change of the particle shape, when applying rescaling. Using the new version of the CEMHYD3D a system resolution of down to 0.2 μm is possible. Garboczi and Bentz [8] point out that 0.2 μm is accurate enough for the simulation of cement hydration and is close to the minimum particle size in cement and other binders [33].

All modifications have been tested for the multi-cycle and multi-scale modification separately, as well as both the modifications combined, for a system consisting of an OPC cement. All simulations showed good agreements between the results at different resolutions (for both methods) and applying different time-steps. The current models are therefore recommended when one wishes to change the system resolution, the cycle-time relation, or both.

Acknowledgements

The authors wish to express their sincere thanks to the European Commission (I-SSB Project, Proposal No. 026661-2) and the following sponsors of the research group: Graniet-Import Benelux, Kijlstra Betonmortel, Struyk Verwo, Attero, Enci, Provincie Overijs-

sel, Rijkswaterstaat Zee en Delta – District Noord, Van Gansewinkel Minerals, BTE, V.d. Bosch Beton, Selor, Twee "R" Recyling, GMB, Schenk Concrete Consultancy, Geochem Research, Icopal, BN International, Eltomation, Knauf Gips, Hess ACC systems, Kronos, Joma, CRH Europe Sustainable Concrete Centre, Cement & BetonCentrum, Heros and Inashco (chronological order of joining).

References

[1] D.P. Bentz, J. Am. Ceram. Soc. 80 (1997) 3.
[2] K. Van Breugel, Simulation of Hydration and Formation of Structure in Hardening Cement-Based Materials, second ed., Delft University Press, Delft, The Netherlands, 1997.
[3] P. Navi, C. Pignat, Adv. Cem. Based Mater. 4 (1996) 58–67.
[4] S. Bishnoi, K.L. Scrivener, Cem. Concr. Res. 39 (2009) 266–274, http://dx.doi.org/10.1016/j.cemconres.2008.12.002.
[5] J.W. Bullard, Model. Simul. Mater. Sci. Eng. 15 (2007) 711–738, http://dx.doi.org/10.1088/0965-0393/15/7/002.
[6] J.W. Bullard, E. Enjolras, W.L. George, S.G. Satterfield, J.E. Terrill, Model. Simul. Mater. Sci. Eng. 18 (2010) 025007, http://dx.doi.org/10.1088/0965-0393/18/2/025007.
[7] W. Chen, H.J.H. Brouwers, Cem. Concr. Compos. 30 (2008) 779–787, http://dx.doi.org/10.1016/j.cemconcomp.2008.06.001.
[8] E.J. Garboczi, D.P. Bentz, Cem. Concr. Res. 31 (2001) 1501–1514, http://dx.doi.org/10.1016/S0008-8846(01)00593-2.
[9] D.P. Bentz, E.J. Garboczi, A digitized simulation model for microstructural development, in: S. Mindess (Ed.), Adv. Cem. Mater. Ceram. Trans., Amer Ceramic Society, 1991. Vol. 16.
[10] D.P. Bentz, Guide to Using CEMHYD3D: A Three-dimensional Cement Hydration and Microstructure Development Modelling Package, NIST, 1997.
[11] R.J. Van Eijk, Hydration of Cement Mixtures Containing Contaminants: Design and Application of the Solidified Product, PhD Thesis, University of Twente, Enschede, The Netherlands, 2001.
[12] W. Chen, Hydration of Slag Cement: Theory, Modeling and Application, PhD Thesis, University of Twente, Enschede, The Netherlands, 2007 <http://doc.utwente.nl/57703/>.
[13] W. Chen, H.J.H. Brouwers, Z.H. Shui, J. Mater. Sci. 42 (2007) 9595–9610, http://dx.doi.org/10.1007/s10853-007-1977-z.
[14] D.P. Bentz, Cem. Concr. Res. 36 (2006) 259–263, http://dx.doi.org/10.1016/j.cemconres.2005.07.003.
[15] S. Igarashi, W. Chen, H.J.H. Brouwers, Cem. Concr. Compos. 31 (2009) 637–646, http://dx.doi.org/10.1016/j.cemconcomp.2009.06.008.
[16] V. Smilauer, Elastic Properties of Hydrating Cement Paste Determined from Hydration Models, PhD Thesis, Czech Technical University, 2005. <http://mech.fsv.cvut.cz/~smilauer/pdf/thesis_smilauer_web.pdf> (accessed 14.04.11).
[17] M. Koster, Mikrostruktur-basierte Simulation des Feuchtetransports in Zement- und Sandstein, PhD-Thesis, RWTH Aachen, 2007 <http://darwin.bth.rwth-aachen.de/opus3/volltexte/2008/2121/> (accessed 02.10.09).
[18] P. Feng, C. Miao, J.W. Bullard, Cem. Concr. Compos. 49 (2014) 9–19, http://dx.doi.org/10.1016/j.cemconcomp.2014.01.006.
[19] N. Robeyst, C.U. Grosse, N.D. Belie, Cem. Concr. Compos. 33 (2011) 680–693, http://dx.doi.org/10.1016/j.cemconcomp.2011.03.004.
[20] D.P. Bentz, CEMHYD3D: A Three-dimensional Cement Hydration and Microstructure Development Modelling Package, version 2.0, NIST, 2000.
[21] D.P. Bentz, CEMHYD3D: A Three-dimensional Cement Hydration and Microstructure Development Modeling Package. version 3.0, NIST, 2005.
[22] D.P. Bentz, Cem. Concr. Compos. 28 (2006) 124–129, http://dx.doi.org/10.1016/j.cemconcomp.2005.10.006.
[23] V. Smilauer, Z. Bittnar, Cem. Concr. Res. 36 (2006) 1708–1718, http://dx.doi.org/10.1016/j.cemconres.2006.05.014.
[24] K. Van Breugel, Cem. Concr. Res. 25 (1995) 522–530, http://dx.doi.org/10.1016/0008-8846(95)00041-A.
[25] A.C.J. De Korte, H.J.H. Brouwers, Chem. Eng. J. 228C (2013) 172–178, http://dx.doi.org/10.1016/j.cej.2013.04.084.
[26] S.H. Berryman, D.R. Franceschetti, Phys. Lett. A 136 (1989) 348–352, http://dx.doi.org/10.1016/0375-9601(89)90413-1.
[27] M. Gardner, Mathematical Circus: More Puzzles, Games, Paradoxes, and Other Mathematical Entertainments from Scientific American with a Preface by Donald Knuth, A Postscript from the Author, and A New Bibliography by Mr. Gardner: Thoughts from Readers, and 105 Drawings and Diagrams, Mathematical Association of America, Washington, DC, 1992.
[28] L.B. Kier, P.G. Seybold, C.-K. Cheng, Cellular Automata Modeling of Chemical Systems: A Textbook and Laboratory Manual, Springer, Dordrecht, 2005.
[29] NIST, Visible Cement Dataset [online], 2002 <http://visiblecement.nist.gov/>.
[30] D.P. Bentz, S. Mizell, S. Satterfield, J. Devaney, W. George, P. Ketcham, et al., J. Res. Natl. Inst. Stand. Technol. 107 (2002) 137–148.
[31] J.W. Bullard, E.J. Garboczi, Cem. Concr. Res. 36 (2006) 1007–1015, http://dx.doi.org/10.1016/j.cemconres.2006.01.003.
[32] A.C.J. de Korte, Hydration and Thermal Decomposition of Cement/Calcium Sulphate based Materials (PhD thesis), Eindhoven University of Technology, Eindhoven, The Netherlands, 2015. <http://repository.tue.nl.dianus.libr.tue.nl/794432>.
[33] M. Hunger, H.J.H. Brouwers, Cem. Concr. Compos. 31 (2009) 39–59, http://dx.doi.org/10.1016/j.cemconcomp.2008.09.010.